

LATERAL CHROMATIC DISPERSION @ CHARA ARRAY: EVALUATION AND POSSIBLE SOLUTIONS

Julien Dejonghe, June-July 2023

The purpose of this document is to determine the principal sources of lateral chromatic dispersion in the CHARA setup, to explain the methods used for measuring, to model the different effects, to discuss the importance of those effects, and to propose technical improvement solutions.

1 Principal sources of lateral chromatic dispersion:

Chromatic dispersion has two distinct origins: **atmospheric differential refraction** when telescopes are going away from zenith, and some **wedged flat optics** present in the coudé beam.

As the amplitude, orientation, and non-linearity of these effects are different and vary in time, we will see that there is no possibility to correct them with a single correcting device, but we will also see that some configurations might be better than other (effect tending to compensate rather than adding themselves).

1.1 Atmospheric Differential Refraction:

At low elevations (or large zenithal distances), the incidence angle between rays coming from the star and atmosphere surface produces a refraction effect. This effect depends on wavelength: the shortest wavelength is, the more light is deviated. In this document, I will more often talk about zenithal distance than elevation, as it is the angle used in Zemax simulations.

A zemax model of the full CHARA optical train and including atmosphere allows to visualize the refraction effect at image plan and LABAO DM plan, for different zenithal angles.

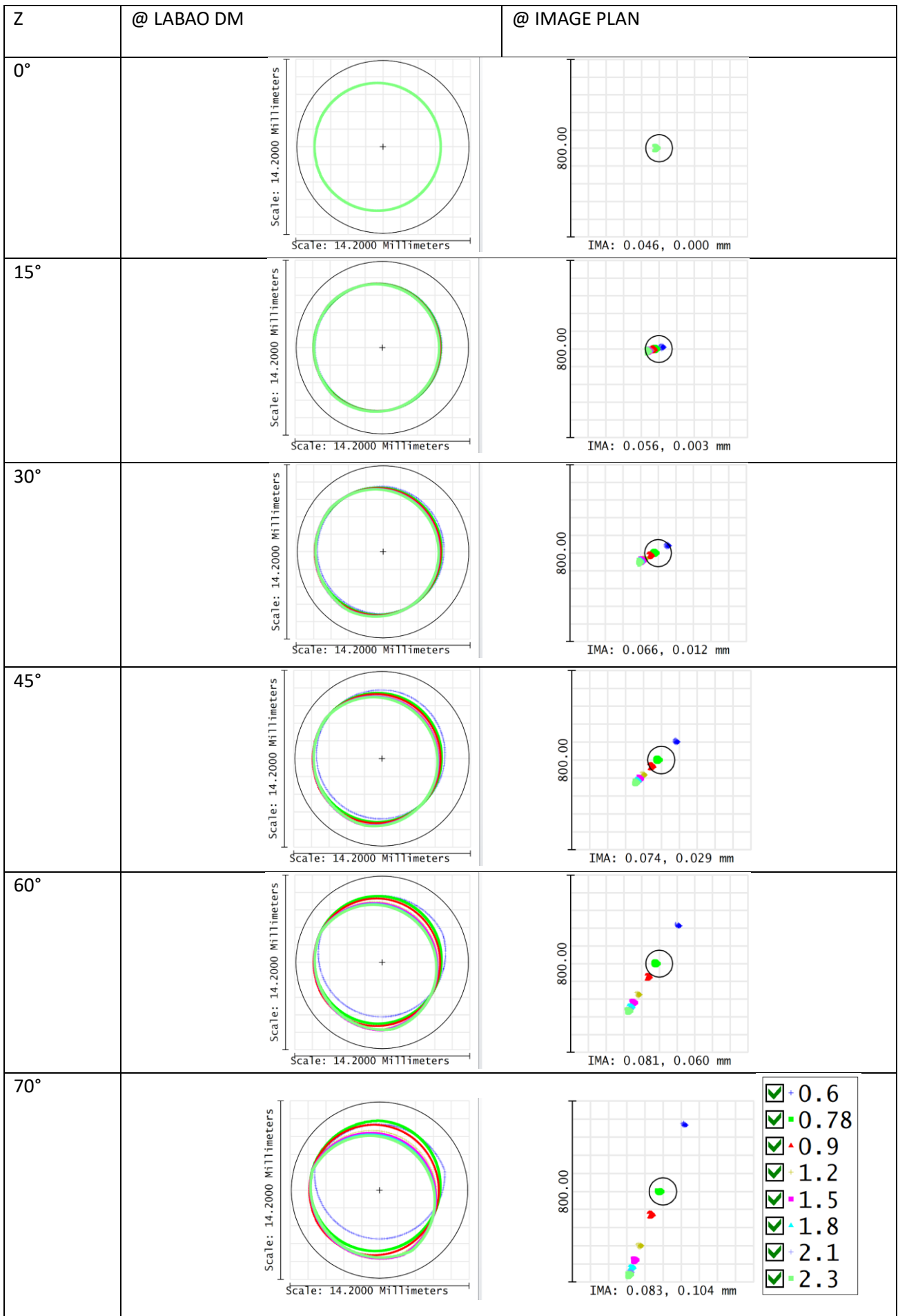
Note that **is this model, there are no other source of dispersion than the atmosphere**. Therefore, it is assumed that the Red Beacon (780nm) is aligned on TWFS with the red light from the star, and that LABAO sees the blue beacon centered but would see the Red Beacon centered as well. This is why it is the 780nm wavelength that appears centered on LABAO DM on the following pictures.

Nevertheless, the beam shift on the DM reaches approximately 13% of its diameter at the lowest elevation (20°), between 780nm and 600nm on the one end, and between 780nm and 2.3 μ m. **From 600nm to 2.3 μ m, the total shift is 26% of the beam diameter.** This might degrade LABAO performance significantly. And this not taking in account wedges effect that will separate Red Beacon and Blue Beacon (450nm), that we will discuss later.

In image plan, the separation between wavelength reaches the size of the Airy disc from 15° (Airy disc shown for 780°, the black circle representing 2.44L/D), reaching 7 to 7 times the Airy disc at 70° of zenithal angle.

Looking closer, we can see that if we consider the NIR wavelength (1.2 μ -2.3 μ), the spot-diagram should be contained in the corresponding Airy disc. The VIS wavelengths are encircled within 3 Airy discs, but this could be corrected by the specific Spica ADC system.

So, it appears that the issues in image plan can be partially managed using Spica internal ADC for the visible, and doing fiber explorer with Mirc-X and Mystic.



- + 0.6
- 0.78
- + 0.9
- + 1.2
- 1.5
- + 1.8
- + 2.1
- 2.3

Fig 1: Atmospheric differential refraction effect @ LABAO DM and @ image plan. **NB: black circle is $1.22\lambda/D@0.78\mu\text{m}$ (red beacon).**

1.2 Dichroic wedges:

Telescopes Dichroics are wedged, to avoid sending any ghost inside the hole of the Acquisition mirror.

1.2.1 Dichro wedge value:

The Acquisition Camera allows to determine the value of the wedge:

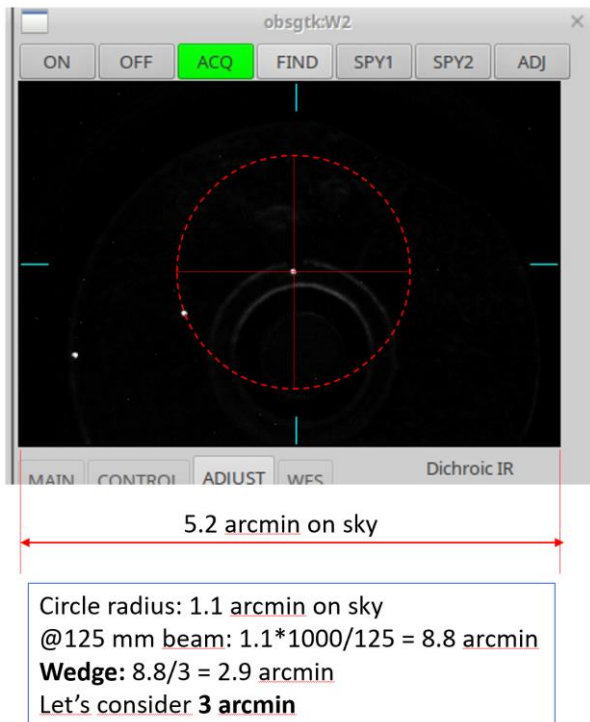


Fig 2: Dichroic wedge evaluation on Acq Camera: **3 arcmin**

1.2.2 Detailed Dichro wedge effect:

A closer look about Dichroic wedge effect shows that we might want pay attention to details:

The Beacon alignment is adjusted so that the Red Beacon appears aligned with the star in TWS. This ensure that the Red Beacon is also aligned with the red star towards the lab. But, as the Beacon light towards lab makes a double path inside the dichroic, the dispersion effect is doubled. Consequently, the Blue Beacon is not aligned with the blue star. **At LABAO DM, the shift from Blue Beacon to Red Beacon (or red starlight) due to the wedged dichroic is approximately 5.4%.**

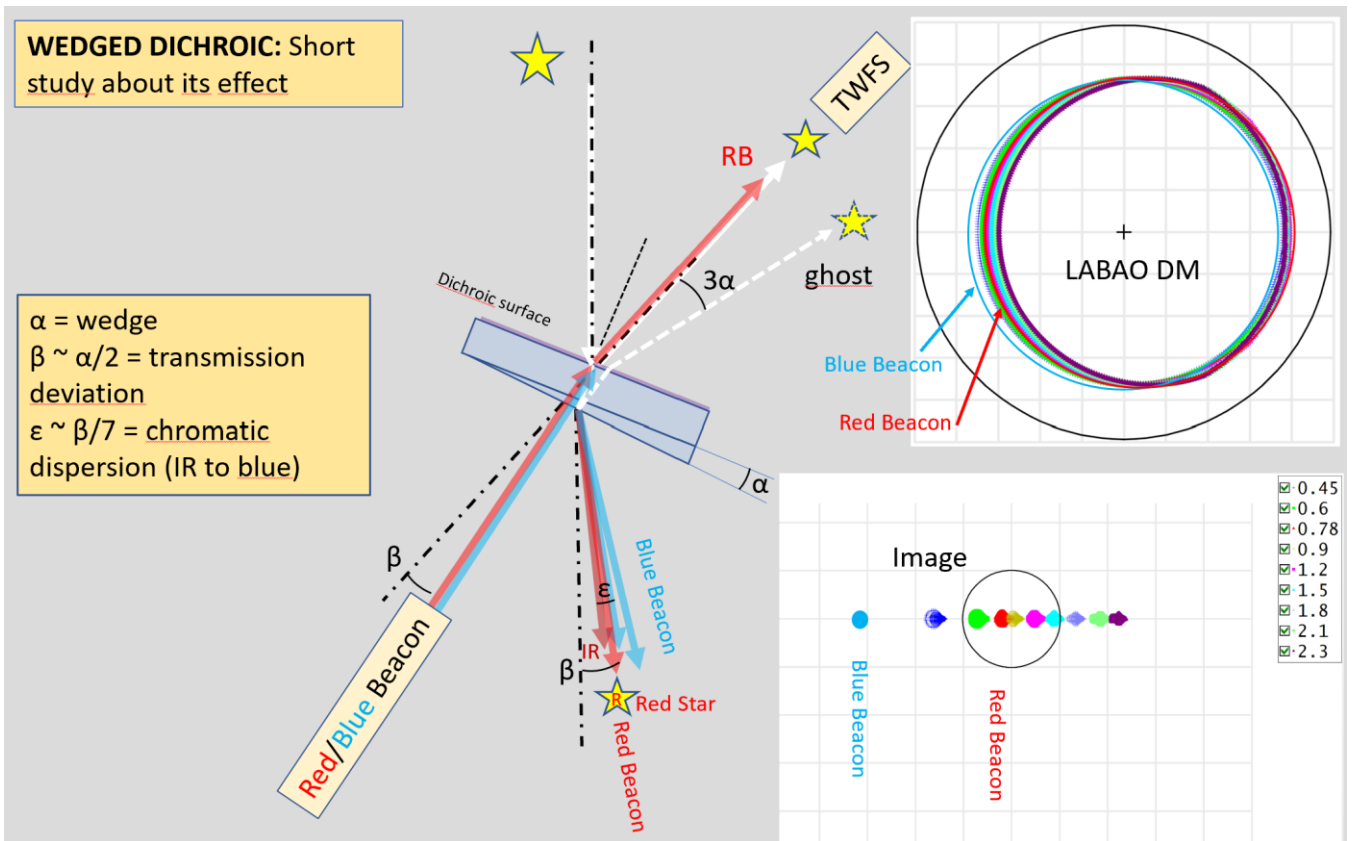


Fig 3: schematic of the Dichro wedge effect on starlight and Red/Blue Beacons. **NB: black circle is $1.22L/D@0.78\mu\text{m}$ (red beacon).**

1.2.3 Current orientation of the wedges:

The direction of the ghosts on the Acq Camera gives us the apex orientation for each telescope, using the method described below:

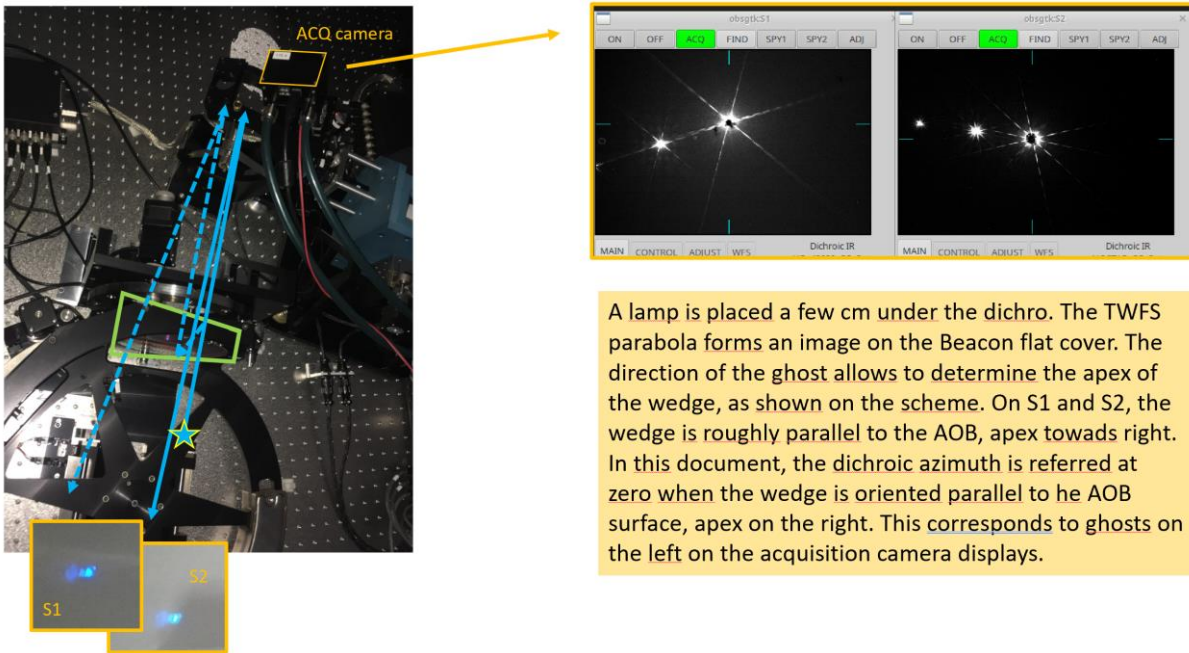


Fig 4: method used to determine the Dichro wedge orientation.

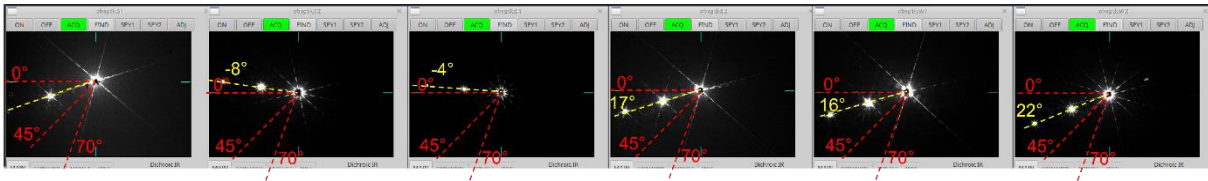


Fig 5: Apex orientation for each telescope, in yellow. In red, orientations that could be useful to minimize the atmospheric effect.

Fig 6: The table below illustrate the current situation, first and second line representing what happens on S2 and E1, the second line W2, W1, E2, S1. The two following lines show that we could improve the situation by orienting the Dichroics either at 45° or 70°. **NB: black circle is 1.22L/D@0.78μm.**

TEL	Wedge az	0°	15°	30°	45°	60°	70°
S2	-8°						
E1							
W2	22°						
W1							
E2							
S1							
similar							
	45°						
	70°						

Of course, this optimization is not a perfect solution, it's only interest is that it is zero cost, pending more complex and expensive improvements we will present later in this paper.

1.3 Wedged Vacuum Windows:

A large part of the CHARA optical path is made in vacuum, for a better stability. The entrance of the vacuum zone is at the lower level of each telescope, near M7. Its exit is in OPLE area, at periscope level, just before M13.

1.3.1 Vacuum windows wedges values and orientation check:

An optical method was used to measure the value of each vacuum window, and to determine the direction of the apex. Ideally, we want the wedge value to be equal and in opposite direction, so it would compensate each other.

A collimated laser source is sent toward the vacuum windows, and a camera with a 200 mm lens gets the light coming back from each faces of the vacuum window. The reflexion from the first surface is seen, as well as the one from the second surface, and the ghost.

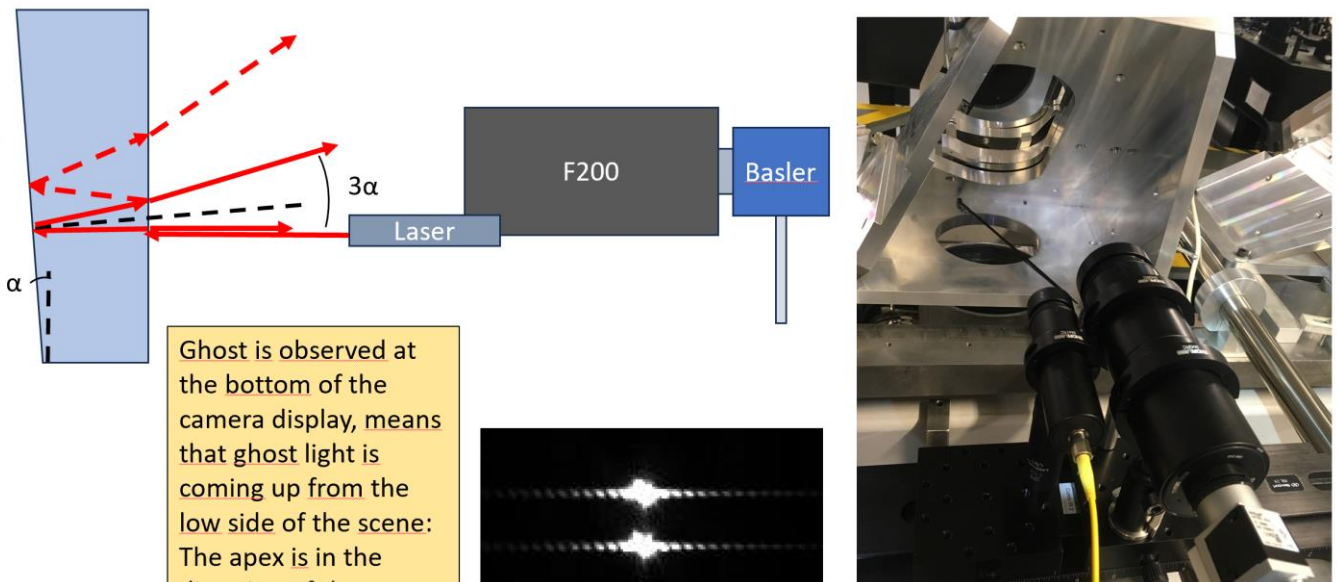


Fig 7: The separation between spots and the orientation allows to determine value and orientation of the vacuum window's wedge.

The Basler camera is oriented in a way that the spots are aligned with the columns of pixels. Then, a thin object is placed into the beam, creating diffraction lines. This object is oriented to get those lines parallel to the pixel lines. In each case, some marks are drawn to materialize the wedge orientation:

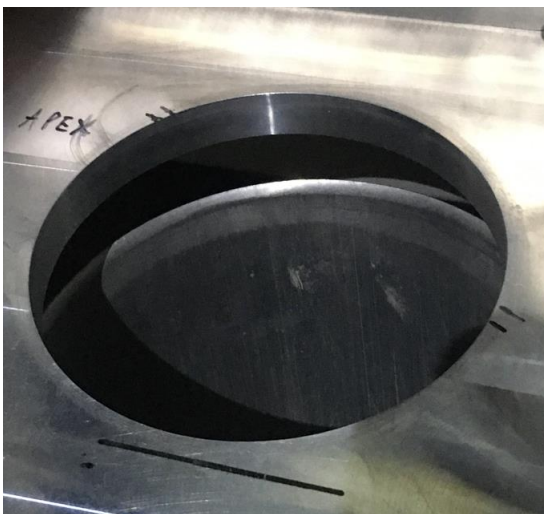


Fig 8: wedge marking (do not erase!).

Each window was measured with the method described below. The estimated accuracy is +/-5%

Fig 9: Different wedge values of the vacuum windows.

Pixel Size (μm)	5.86	Focal Length:	200 mm			
$200 \times 3 \times \text{wedge} = \text{Nb pix} \times 0.00586$						
Wedge = $0.00000976 \times N$ (rad)						
Wedge = $2.018 \times N$ (arcsec)						
TELESCOPE	Wedge at LAB			Wedge at TEL		
	Pixels	Arcsec		Pixels	Arcsec	
S1	21	42	23	46		
S2	19	38	24	48		
W1	18	36	20	40		
W2	25	50	21	42		
E1	20	40	21	42		
E2	18	36	21	42		

1.3.1.1 *Relative wedge orientation:*

As understood, the wedge values are similar, but in order to compensate for themselves, the Vacuum Windows wedges should be oriented in opposite direction, when projected from the entrance to the exit.

The method used to determine the relative orientation for each line is described below:

First, an arrow materializing the entrance window apex is placed above M7, and enlighten with a lamp and a white diffusing paper (not on this photo). The arrow is in the direction of the apex. The same thing is done for the exit window.



Fig 10: Arrows materializing the vacuum wedges, at entrance (left), and exit (right).

Then, a small telescope is placed on the Cart rails, near the periscope, and facing towards the Cart:



Fig 11: Celestron telescope on the rails.

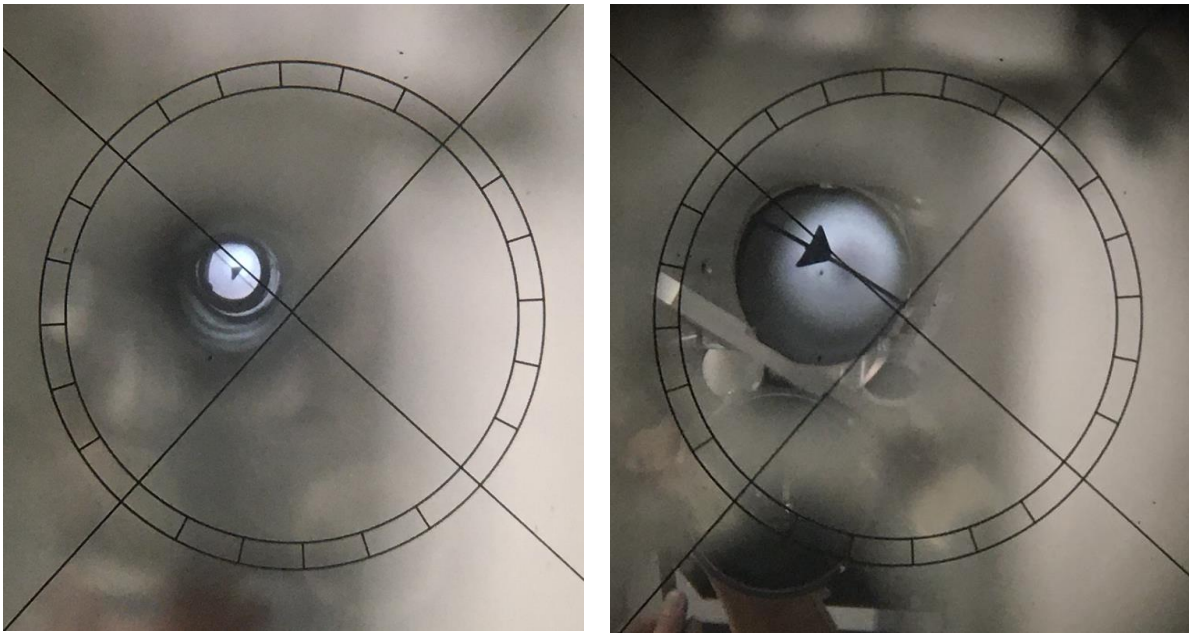
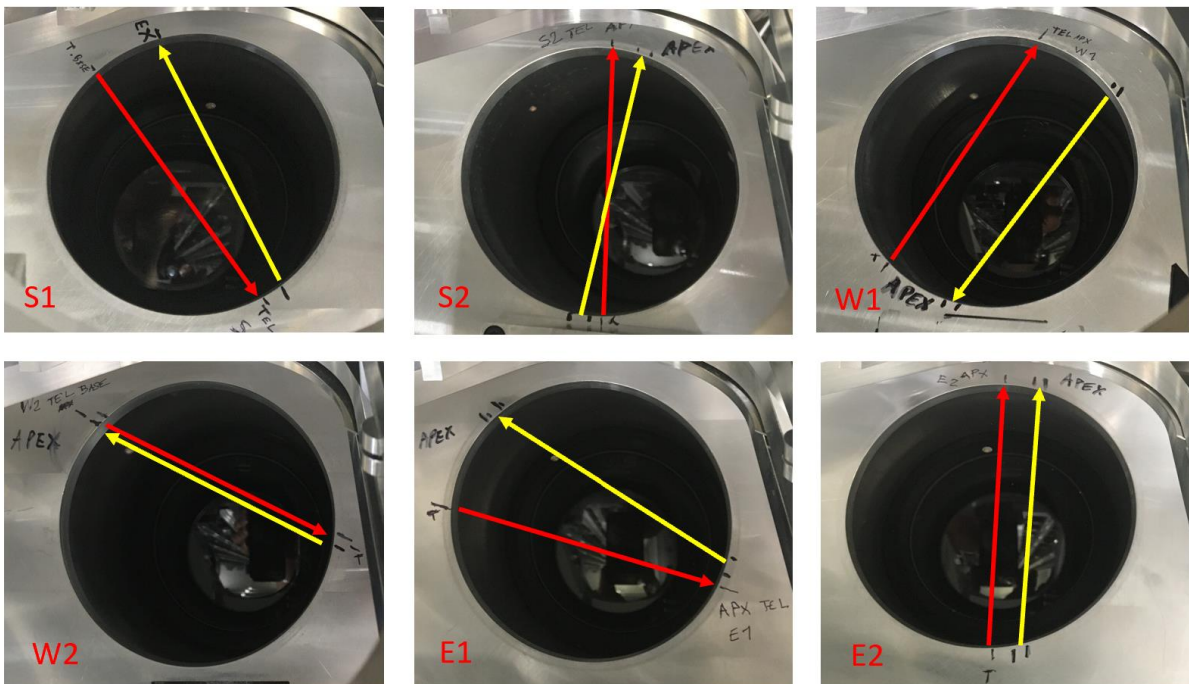


Fig 12: Focusing the telescope allows to see either entrance (left) or exit (right) vacuum windows. Here, the direction are opposed as required, but a small orientation error is observed.

For each line, the reticle is oriented parallel to the entrance arrow, then the exit windows arrow is oriented manually to be parallel to the reticle axis. Finally, some marks are done on the periscope mechanics to indicate the respective orientation of the vacuum windows, as shown below:



Red: entrance; Yellow: exit

S1: good – S2: wrong – W1: perfect – W2: perfect – E1: nearly good – E2: wrong

Fig 13: illustration of the Vacuum Windows wedges for each line.

1.3.2 Effects of the wedged Vacuum Windows:

A Zemax model of the CHARA optical train is used to determine whether the dispersion caused by the vacuum windows wedges is a problem or not. In this simulation, telescope is at zenith, and there is no wedge at the dichroic.

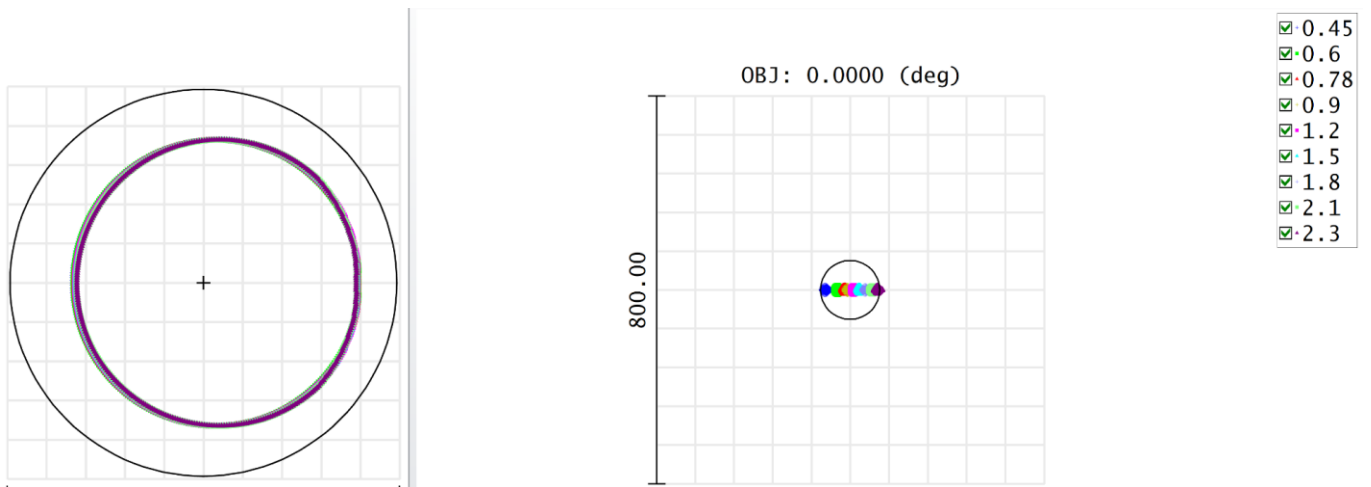


Fig 14: Vacuum Windows wedge effect in the worst case (**S2**: wedges are in the same direction), on LABAO DM (left) and image (right). **NB: black circle is $1.22\lambda/D$ @ $0.78\mu\text{m}$ (red beacon).**

We can see that the beam shift on LABAO DM is negligible, meanwhile the shift in image plane is the size of the Airy disc of the red beacon.

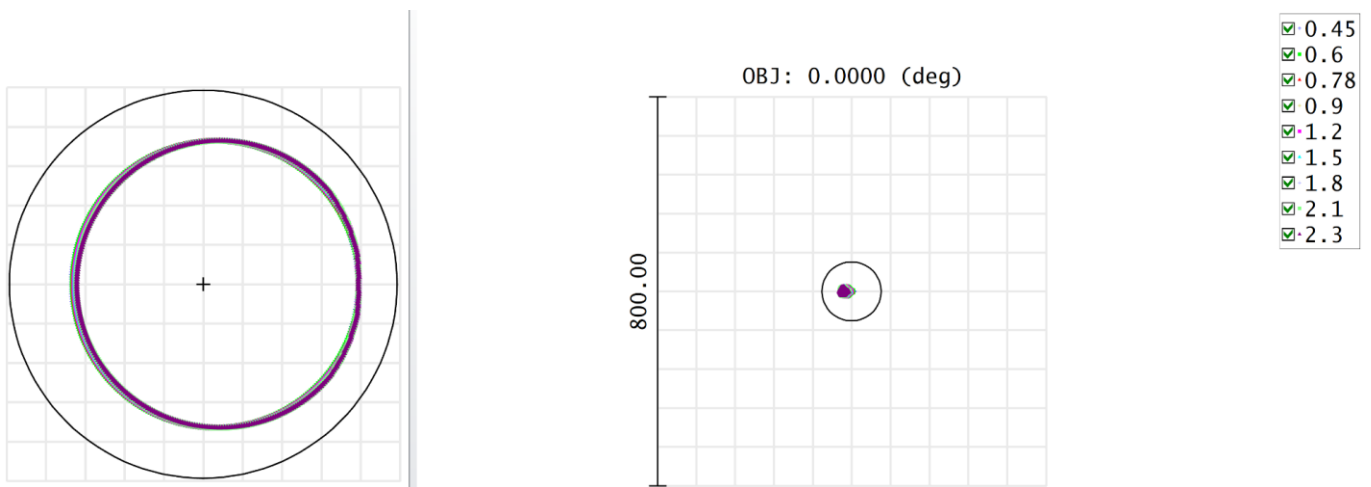


Fig 15: Vacuum Windows wedge effect in a good case (**W2**), on LABAO DM (left) and image (right).

2 Improvement proposals:

The amplitude, orientation, and non-linearity of the effects presented earlier are different and vary in time, there is no possibility to correct them with a single correcting device. Nevertheless, avoiding cumulative effects could be appreciated. We will see below different solutions to reduce each disturbing effect.

2.1 Wedged Vacuum Windows:

This effect is negligible at LABAO DM, but for S2 and E2, the dispersion in image plan is about the Airy disc size, so a simple 180° rotation of the exit vacuum window for those lines could easily improve the situation, and this operation would be costless.

A rapid check of a non-perfect situation like E1 show a small improvement in image is possible by turning the exit window of about 30°:

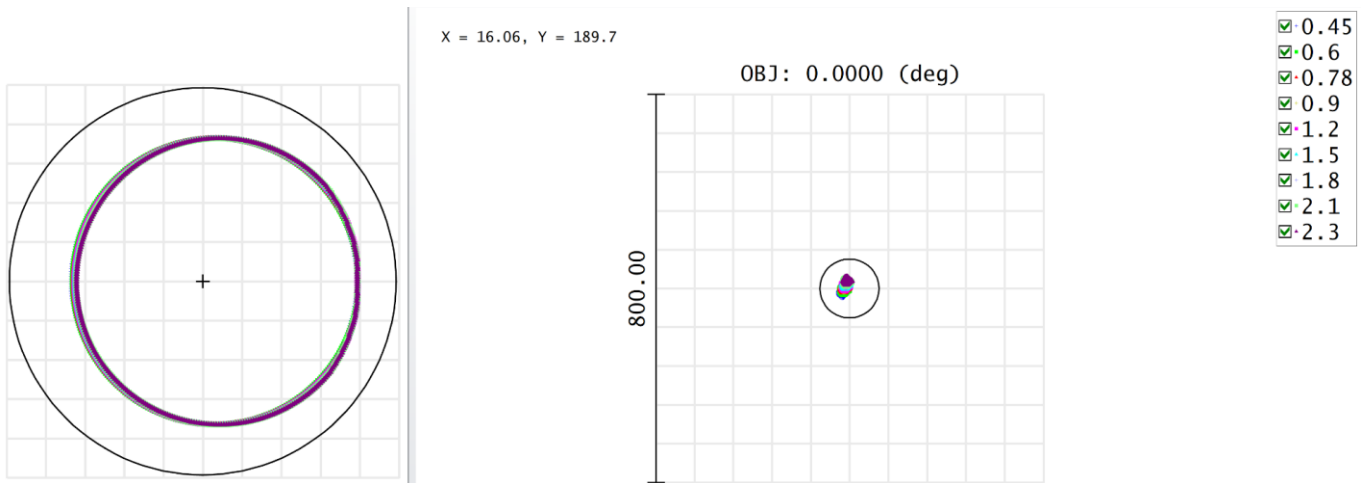


Fig 16: current situation for E1.

2.2 Wedged Telescope Dichroic:

As shown in section 1.2.3, the wedge of the telescope dichroic disperses the light significantly:

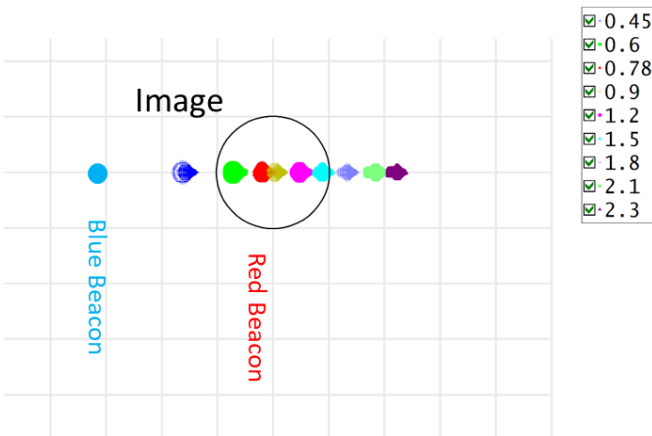


Fig 17: dispersion due to wedged dichroic.

This effect is complicated by the fact that the light from the red and blue beacons is dispersed twice more than the starlight due to a double-pass. CHARA has the particularity to work from red to near infra-red for science, but to be aligned in blue (blue beacon 450 nm). Replacing the blue beacon with a 950 nm source could improve the situation, allowing to align with a wavelength better centered in the science band:

2.2.1 A new 950 nm beacon?

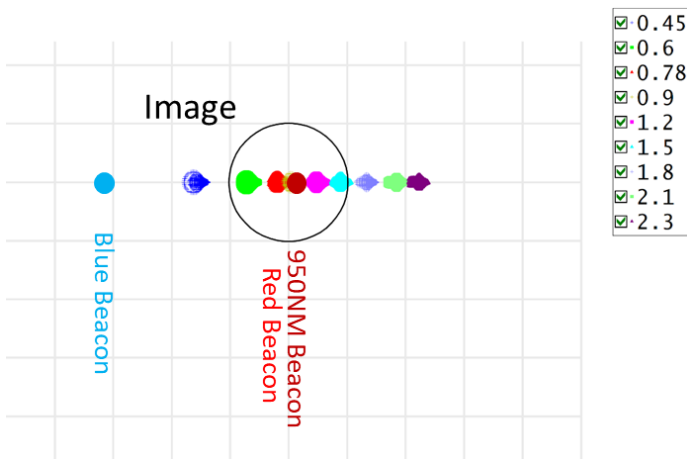


Fig 18: a 950 nm beacon better centered in the scientific band.

The following illustration represents the VIS and IR Dichroics T/R curves, and the current transmitted or reflected light from blue and red beacon, and for a possible 950 nm beacon. This modification would imply a new filter for TWFS, probably the replacement of the LABAO detector, a custom beamsplitter for LABAO, and a refocusing of LABAO setup, as listed in the figure.

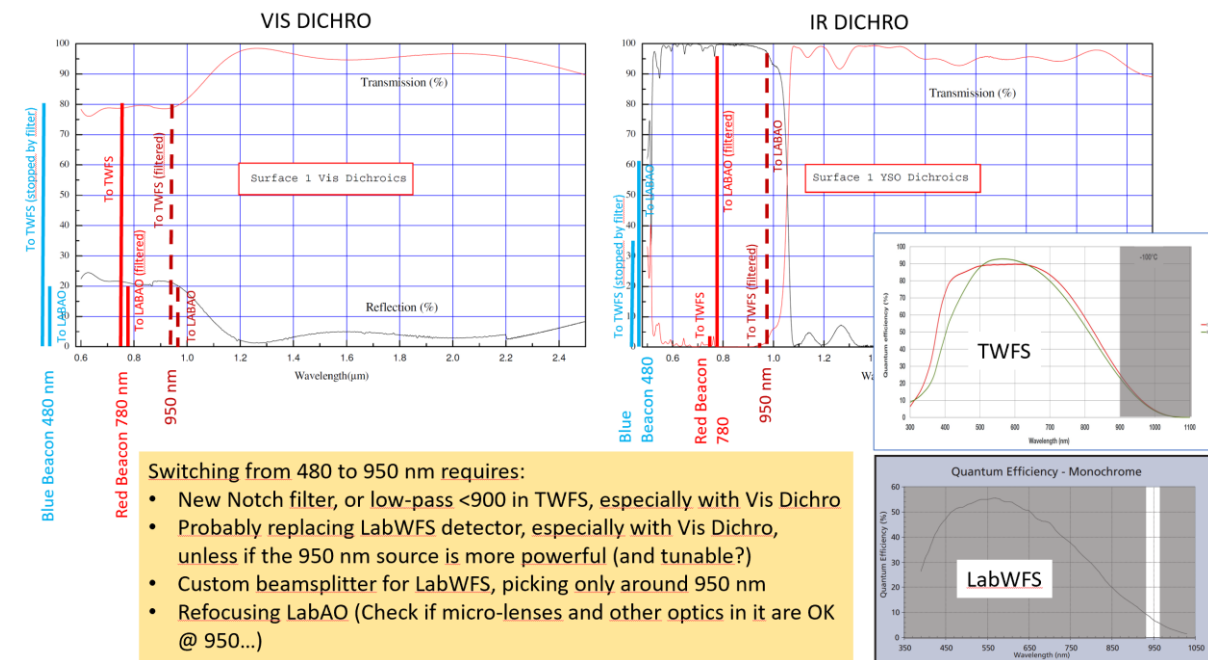


Fig 19: VIS/IR Dichroics T/R curves, and transmitted or reflected light from different beacons.

2.2.2 Reducing the wedge of the Telescope Dichroic?

The current wedge of the Telescope Dichroic is typically 3 arcmin.

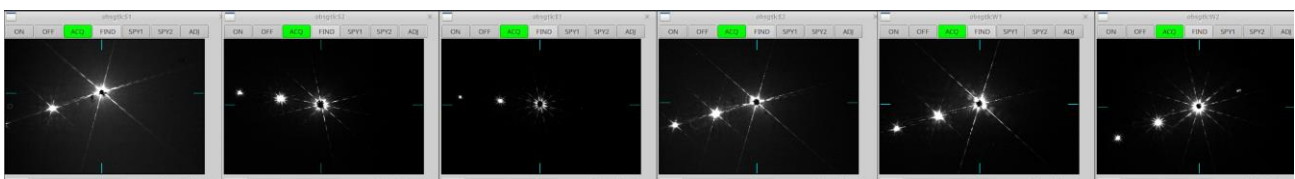


Fig 20: The ghosts on the Acq camera shows that all wedges values are similar, a bit larger for S1, and we can notice that the first ghost is quit far away from the hole, so an option could be to reduce the wedge to 1 arcmin.

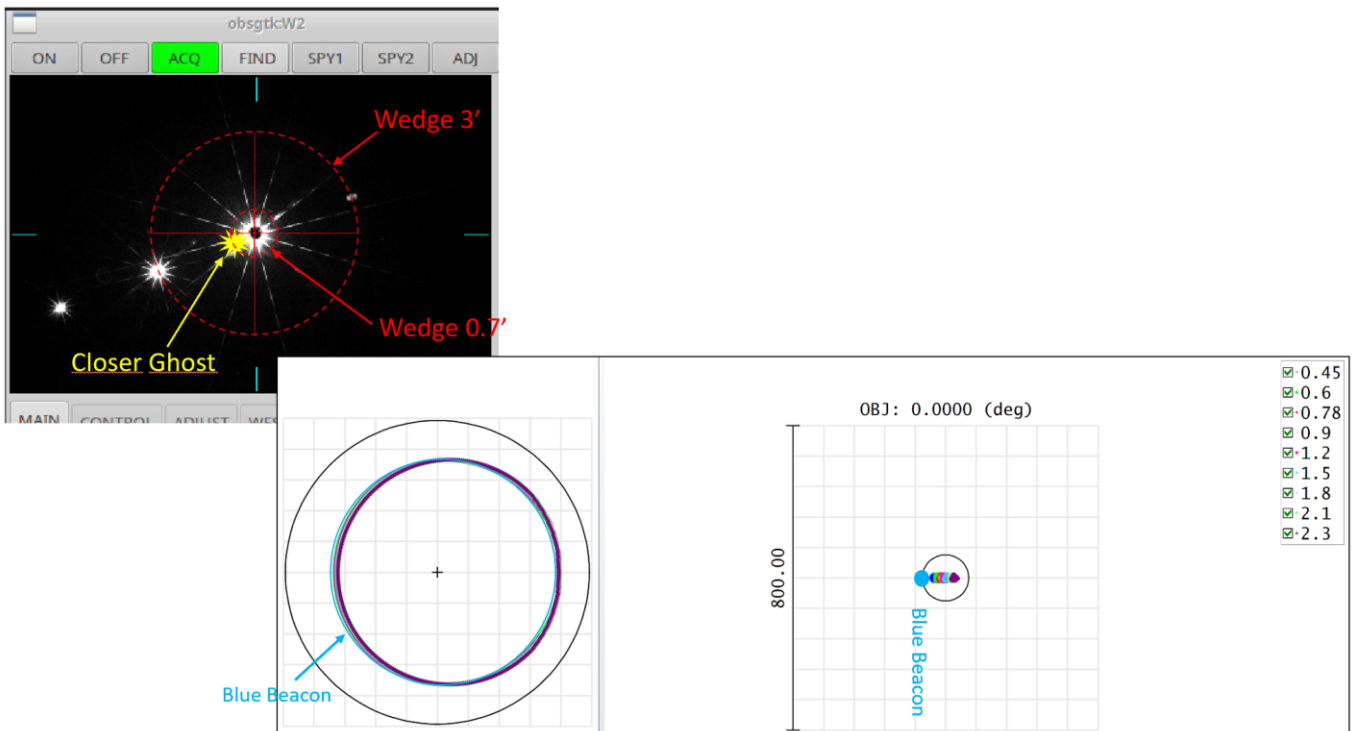


Fig 21: The situation with a 0.7' reduced Dichroic wedge. Beam shift at LABAO DM is 2% approximately, and science light is maintained inside the Airy disc. If this option would be retained, we must be sure that there is not too much ghost light going to the TWFS.

2.2.3 Telescope Dichroic wedge compensator?

To compensate the dispersion effect of the wedged dichroic on starlight, a second opposed wedged window could be placed after it, before M5. That would completely negate the effect for starlight, but only “half-negate” the effect for beacon light (no double pass in the second window). In this situation, the Blue Beacon beam should be shifted from starlight of 2.7% at LABAO DM.

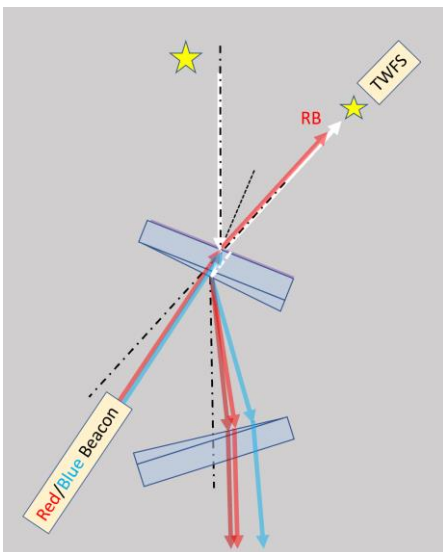


Fig 22: a second wedge to compensate the effects of the first one. The starlight is not dispersed anymore, but the separation between red and blue beacon is only halved.

The BARE dichroic is not used for science, so maybe it could be removed from the Carousel, and be used as a compensator. Both faces would have to be anti-reflection coated, from 0.6 to 2.4 μm .

2.2.4 Optimizing Telescope Dichroic azimuth?

This was already discussed in section 1.2.2, Fig 6.

2.3 Correcting atmospheric differential refraction:

Atmospheric Differential refraction correctors (ADC) are optical devices designed to compensate the lateral dispersion due to atmosphere.

2.3.1 ADC classical design:

A classical design used in collimated beams consists in two Risley prisms. A Risley prism is a double prism made with two different glasses, with different refraction index. Having two different glasses allows to have a dispersion effect, like with a single prism, but without global deviation. The combination of two Risley prisms oriented in adjustable manner in opposite ways regarding the atmospheric dispersion acts as if we had a single Risley prism but with adjustable wedges angles.

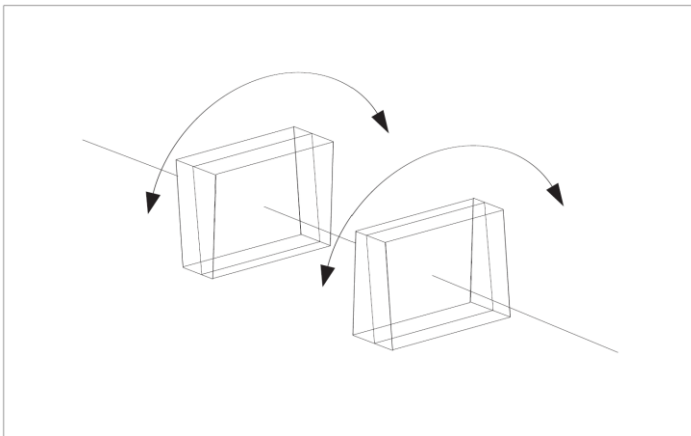


Fig 23: Principle of an ADC composed of two Risley prisms.

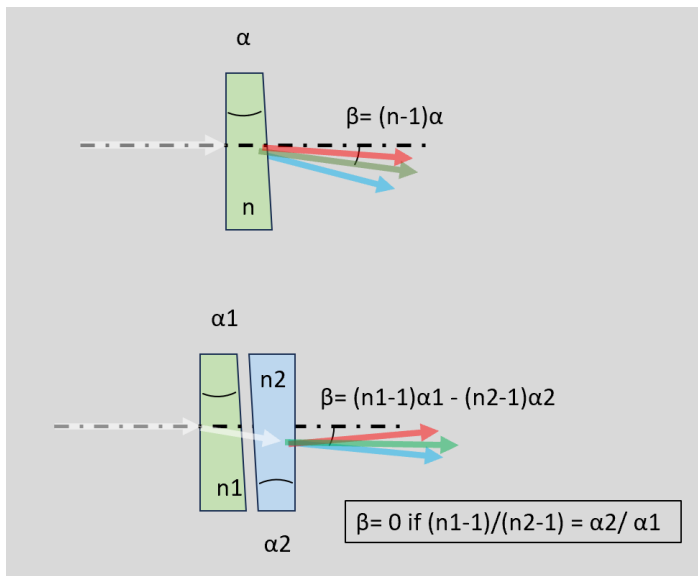


Fig 24: principle of a zero-deviation prism.

The first step is to determine which glasses are adapted to our requirements:

- Good transmission from 0.6 to 2.3 μm
- Good resistance to humidity
- No birefringence

In practice, a Zemax model was used to converge in a correct ADC optical design:

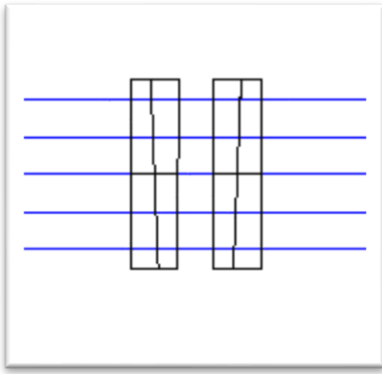


Fig 25: view of the Zemax model.

The merit function used in this Zemax model contains operands relative to the spot position for each wavelength, and other operands relative to transmission for each wavelength. By playing with the weight given to those operands, the optimization process will converge either to a solution for the best transmission, or for the best dispersion correction. Zemax algorithm allows to automatically pick some glasses in a catalog, and makes varying the two prisms angles.

Merit Function Editor

Wizards and Operands Merit Function: 0.003233770061786

Type	Surf	Wave	Hx	Hy	Px	Py	Targ	Weight	Value	% Contrib	
1	BLNK	ZERO DEV									
2	REAY	14	1	0.000	0.000	0.000	0.000	10.000	3.588E-03	17.570	
3	REAY	14	2	0.000	0.000	0.000	0.000	10.000	-2.426E-03	8.034	
4	REAY	14	3	0.000	0.000	0.000	0.000	10.000	-3.658E-03	18.258	
5	REAY	14	4	0.000	0.000	0.000	0.000	10.000	-3.043E-03	12.640	
6	REAY	14	5	0.000	0.000	0.000	0.000	10.000	-1.168E-03	1.861	
7	REAY	14	6	0.000	0.000	0.000	0.000	10.000	1.947E-03	5.172	
8	REAY	14	7	0.000	0.000	0.000	0.000	10.000	4.803E-03	31.482	
9	BLNK	TRANSMISSION									
10	CODA	0	1	1	0	0.000	0.000	1.000	1.000E-02	0.984	0.346
11	CODA	0	2	1	0	0.000	0.000	1.000	1.000E-02	0.980	0.524
12	CODA	0	3	1	0	0.000	0.000	1.000	1.000E-02	0.984	0.353
13	CODA	0	4	1	0	0.000	0.000	1.000	1.000E-02	0.987	0.233
14	CODA	0	5	1	0	0.000	0.000	1.000	1.000E-02	0.983	0.378
15	CODA	0	6	1	0	0.000	0.000	1.000	1.000E-02	0.973	1.010
16	CODA	0	7	1	0	0.000	0.000	1.000	1.000E-02	0.960	2.139

Fig 26: the Merit Function.

The Schott catalog was used to try to find suitable glasses. Giving priority to transmission gave the following spot-diagram, with N-PK52A and N-FK58 glasses.

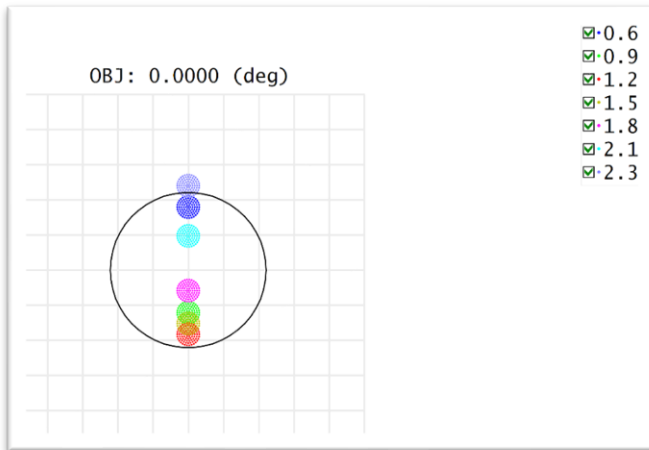


Fig 27: N-PK52A and N-FK58 glasses.

Giving priority to dispersion gave the following spot-diagram, with N-PK51 and N-FK58 glasses.

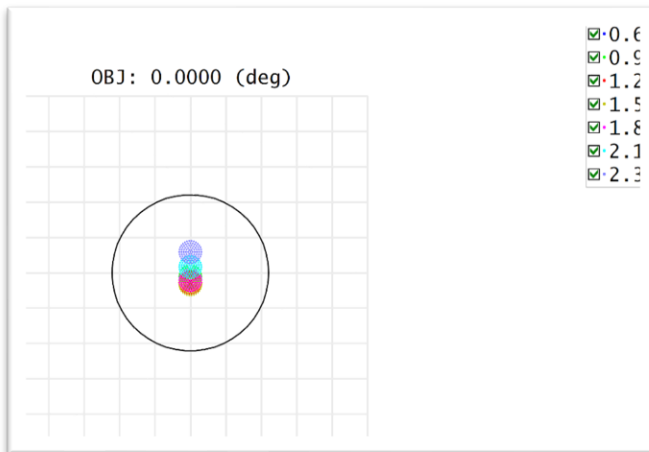


Fig 28: N-PK51 and N-FK58 glasses.

Wavelength (nm):	Internal transmission (25mm)						
	2325	1970	1530	1060	700	660	620
N-PK51	0.860	0.966	0.985	0.994	0.992	0.991	0.992
N-PK52A	0.978	0.990	0.994	0.994	0.993	0.993	0.995
N-FK58	0.996	0.998	0.998	0.995	0.993	0.993	0.994

Fig 29: extract from SCHOTT glass catalog. Those 3 glasses are class 1 climatic resistance (best resistance).

ZEMAX TRANSMISSION SIMULATION (perfect coatings)		
T% (4 prisms 20mm thick)		
Wavelength (μm):	Priority dispersion	Priority transmiss
	N-PK51 N-FK58	N-PK52A N-FK58
0.6	9.80E-01	9.84E-01
0.9	9.80E-01	9.80E-01
1.2	9.80E-01	9.84E-01
1.5	9.74E-01	9.87E-01
1.8	9.55E-01	9.83E-01
2.1	8.82E-01	9.73E-01
2.3	7.92E-01	9.60E-01

Fig 30: Transmission of the ADC calculated by Zemax.

2.3.2 Another type of ADC?

The system presented above consists in 4 prisms and 2 different glasses. This is necessary to have a zero-deviation system.

Another solution could be to have 2 prisms made of the same glass, and disposed close to M4 (Tel DM). The deviation caused by the ADC could be compensated by orienting slowly M4, as shown on the scheme below:

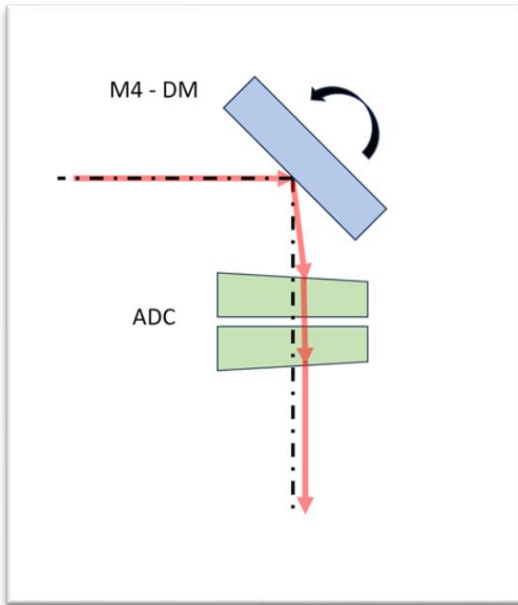


Fig 31: ADC with 2 prisms made of the same glass and a mirror compensating for the deviation.

A suitable glass compensating correctly the atmosphere have to be found.

To be continued....